SYNTHESIS OF NATURAL ADSORBENTS FROM LIGNOCELLULOSIC BIOMASS FOR THE RECOVERY OF BORON FROM WATER RESOURCES

A Thesis Submitted to
the Graduate School of Engineering and Sciences of
İzmir Institute of Technology
in Partial Fulfillment of the Requirements for the Degree of

MASTER OF SCIENCE

in Chemical Engineering

by
Bekir Fırat ALTINBAŞ

July 2023
İZMİR

We approve the thesis of **Bekir Fırat ALTINBAŞ**

Examining Committee Members:

_____

Assoc. Prof. Dr. Aslı YÜKSEL ÖZŞEN
Chemical Engineering Department, Izmir Institute of Technology

_____

Assoc. Prof. Dr. Ayben TOP
Chemical Engineering Department, Izmir Institute of Technology

_____

Assoc. Prof. Dr. Canan URAZ
Chemical Engineering Department, Ege University

4 July 2023

_____

Assoc. Prof. Dr. Aslı YÜKSEL ÖZŞEN
Supervisor, Chemical Engineering Department,
Izmir Institute of Technology

_____   _____

Prof. Dr. Erol ŞEKER   **Prof. Dr. Mehtap EANES**
Head of the Department of Chemical Engineering   Dean of the Graduate School
of Engineering and Sciences

ACKNOWLEDGMENTS

I would like to express my deepest gratitude to my advisor, Assoc. Prof. Dr. Aslı Yüksel Özşen, for her continuous guidance, unwavering support, and belief in me throughout my thesis project. Thank you for allowing me to be a part of this endeavor.

I am truly grateful for the amazing support and guidance provided by the Yuksel Research Group members, especially during lab experiments. Your contributions have been invaluable to my success, alongside my advisor. Thank you so much!

I would like to thank Izmir Institute of Technology Integrated Research Centers, namely Geothermal Energy Research and Application Center (GEOCEN), Biotechnology and Bioengineering Application and Research Center and Environmental Development, Application and Research Center, for characterization analyses of cellulose-based adsorbents and boron analysis.

I would like to take this opportunity to express my heartfelt appreciation to my beloved mother. Her constant love and unwavering support have been the driving force behind my success. I am forever grateful for her guidance and encouragement, which have helped me overcome many obstacles in life. Thank you, Mom, for being my rock and always believing in me.

ABSTRACT

SYNTHESIS OF NATURAL ADSORBENTS FROM LIGNOCELLULOSIC BIOMASS FOR THE RECOVERY OF BORON FROM WATER RESOURCES

This work investigated the valorization of olive tree pruning waste as a biosorbent for the removal of environmentally hazardous boron from aqueous solution using batch adsorption. For this purpose, a novel, waste-based, boron-selective biosorbent from pristine cellulose and olive tree pruning waste (N-OPW) was synthesized. After confirming the proposed synthesis route with pristine cellulose, an alkali pretreatment, followed by glycidyl-methacrylate (GMA) grafting and providing boron selectivity with n-methyl-d-glucamine (NMDG) steps were applied to the biomass, respectively. N-OPW was characterized using SEM, TGA and FT-IR analyses. N-OPW showed excellent boron biosorption capacity (21.80 mg/g) in an operation pH range between 2-12. The equilibrium was attained in two hours and the Freundlich isotherm (R^2=0.997) and pseudo-second-order kinetics (R^2=0.99) provided the strongest match to experimental data. According to thermodynamic studies, boron adsorption was exothermic ($\Delta H°$= -34.14 kJ/mol). The reusability tests with real geothermal water showed that adsorbent had no significant decrease in boron removal capacity while desorbing >99% of the boron adsorbed for three cycles of adsorption/desorption. Results indicated that a promising, reusable, and boron-selective biosorbent was successfully synthesized while utilizing olive pruning waste.

ÖZET

SU KAYNAKLARINDAN BOR GİDERİMİ İÇİN LİGNOSELÜLOZİK ATIKLARDAN DOĞAL ADSORBANLARIN SENTEZLENMESİ

Bu çalışmada, zeytin ağacı budama atığının, çevresel olarak tehlikeli boru, sulu çözeltilerden adsorpsiyon yoluyla uzaklaştırılmak için bir biyosorbent olarak değerlendirilmesi araştırılmıştır. Bu amaçla, saf selüloz ve zeytin ağacı budama atığından oluşan yeni bir, atık temelli, bor seçici bir biyosorbent (N-OPW) sentezlenmiştir. Önerilen sentez yolunun saf selüloz ile doğrulanmasının ardından, zeytin ağacı budama atığına sırasıyla alkali ön işleme, glisidil-metakrilat (GMA) aşılama ve n-metil-d-glukamin (NMDG) ile bor seçiciliği sağlama adımları uygulanmıştır. Elde edilen adsorbent, SEM, TGA ve FT-IR analizleri kullanılarak karakterize edilmiştir. N-OPW, 2-12 arasındaki işletim pH aralığında mükemmel bir bor adsorpsiyon kapasitesi (21.80 mg/g) göstermiştir. Adsorpsiyon dengesi iki saatte sağlanmış, ve Freundlich izotermi (R^2=0.997) ve ikinci dereceden psödo-kinetik model (R^2=0.99) deneysel verilerle en iyi eşleşmeyi sağlamıştır. Termodinamik çalışmalara göre, bor adsorpsiyonu ekzotermiktir ($\Delta H°$= -34.14 kJ/mol). Gerçek jeotermal su ile yapılan yeniden kullanılabilirlik testleri, adsorbanın üç adsorpsiyon/desorpsiyon döngüsü için adsorbe edilen borun %99'dan fazlasını desorbe ederken borun uzaklaştırma kapasitesinde önemli bir azalma olmadığını göstermiştir. Sonuçlar, zeytin budama atığından faydalanırken umut verici, yeniden kullanılabilir ve bor seçici bir biyosorbentin başarıyla sentezlendiğini göstermektedir

TABLE OF CONTENTS

LIST OF FIGURES

LIST OF TABLES

LIST OF ABBREVIATIONS

M_{ads}	Mass of adsorbent
GMA	Glycidyl methacrylate
NMDG	N-methyl-d-glucamine
BPO	Benzoyl peroxide
CMS	Microcrystalline Cellulose Microsphere
TGA	Thermogravimetric Analysis
SEM	Scanning Electron Microscopy
FTIR	Fourier Transform Infrared Spectroscopy
ΔH^o	Standard enthalpy change
ΔS^o	Standard entropy change
ΔG^o	Gibbs free energy
T	Temperature
q_e	Adsorbed boron amount at equilibrium (mg/g)
q_{max}	Maximum adsorption capacity (mg/g)
OPW	Olive pruning waste
AT-OPW	Alkali-treated olive pruning waste
G-OPW	Glycidyl methacrylate grafted olive pruning waste
N-OPW	NMDG attached olive pruning waste

CHAPTER 1

INTRODUCTION

Boron is a critical component of many industries, including glass, fertilizers, electronics, and detergents [1], and the widespread use of boron compounds results in the release of boron-contaminated water. Also, the processing of geothermal brine in geothermal plants result in boron contaminated effluents since geothermal brine naturally contains boron species [2]. Controlling the amount of boron in drinking and irrigation water is crucial due to its toxicity for both plants and people [3]. In 2011, the World Health Organization (WHO) approved boron levels in drinking water and irrigation water of up to 2.4 and 1.0 mg/L, respectively [4]. Therefore, it is critical from an environmental standpoint to remove boron from used solutions and geothermal brine. Depending on the boron species' size and charge, various boron removal methods can be utilized. Rather than eliminating boron from aqueous solutions, methods such as extraction, crystallization or evaporation are employed to produce boric acid [5].

Boron removal technologies that are commonly employed include adsorption, ion exchange, reverse osmosis, nanofiltration, chemical, and electrocoagulation. These strategies are also employed as hybrid systems [5]–[8]. However, in terms of cost and convenience of use, adsorption is thought to be a viable method to eliminate boron from aqueous solutions. [9].

To be used in adsorption process, commercial adsorbents with boron selectivity are derived mostly from polystyrene, a petroleum-based support material. Since the synthetic supports are non-biodegradable, long term usage results in environmental damage. Thus, the replacement of the support material with a low-cost, ecologically friendly substance remains as a gap in the literature. Replacement of the support material with ecologically friendly materials such as cellulose from waste biomass, is a potential alternative for long-term sustainability by elimination of waste biomass while preventing usage of synthetic materials [10], [11]. Cellulose contains three hydroxy groups that can be modified to obtain different types of cellulosic material, that can be utilized for synthesis of a selective adsorbent. Among various cellulose sources, lignocellulosic biomass, such as rice and

coffee husks, walnut shells [9], [12] had gained interest as biosorbents. In literature, to remove boron, lignocellulosic biomasses such as banana peels [13] (boron removal capacity of 3.9 mg/g), olive bagasse-derived activated carbon [14] (boron removal capacity of 3.5 mg/g) are used without any modification, resulting to a relatively low boron removal capacity compared to commercial boron adsorbents like Diaion CRB02 and CRB05 (13.18 and 17.45 mg/g). Therefore, indicating that modification of lignocellulosic biomass before utilizing it as a biosorbent with high removal capacity is necessary. Thus, a novel boron selective adsorbent can be synthesized by utilizing a renewable cellulose source such as lignocellulosic biomass to selectively remove boron.

In this context, olive pruning waste (OPW) was utilized for production of a novel cellulose-based adsorbent with n-methyl-d-glucamine (NMDG) functional group. Due to -OH groups of NMDG that can form mono and bis-chelate complexes selectively with boron species as shown in Figure 1 below, the functional group is suitable for boron removal [15].
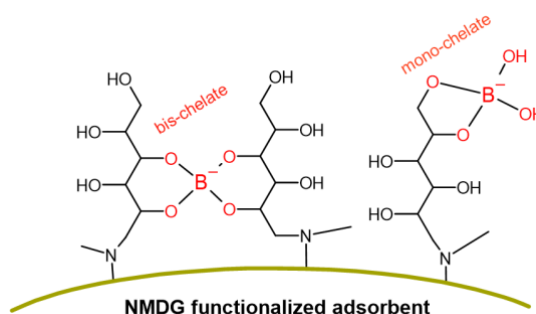
Figure 1. Adsorption mechanism of boron species onto NMDG type adsorbents

After applying the proposed method to pristine cellulose, the procedure was applied to olive tree pruning waste. Before the modification of OPW, an activation process to expose more -OH groups in the biomass structure were applied before chemical modification reactions using an alkali treatment method. Graft polymerization of cellulose with glycidyl-methacrylate (GMA) was utilized for preparing the adsorbent surface for anchoring NMDG group onto the adsorbent since epoxy rings of GMA can host a variety of functional groups [4]. Also, previous studies of NMDG group-based

2

adsorbents prepared with cellulose-GMA complex show remarkable boron removal capacities [16]–[18].

SEM, TGA, FT-IR and elemental analyses along with determination of pH_{PZC} of the adsorbent were carried out to characterize the synthesized adsorbent, while batch experiments were used to investigate the impacts of important adsorption factors for boron removal such as pH and adsorbent dosage. Adsorption kinetics, isotherms and thermodynamics were studied. Three consecutive adsorption/desorption cycles using real geothermal water were done to assess reusability of the synthesized adsorbent.

CHAPTER 2

LITERATURE REVIEW

2.1. Importance of Boron

While boron is an essential micronutrient and a useful component for various industries, it becomes toxic after the boron amount exceeds the required amount and the safe band of boron content in aqueous solutions is very narrow, for example, the sunflower plant needs 0.5 ppm boron while 1 ppm is toxic for the plant [19]. Therefore, the amount of boron present in the aqueous solutions is very crucial for applications.

2.2. Boron Sources and Boron in Aqueous Solution

Boron is present in nature at earth's lithosphere and hydrosphere in rocks, and soils in earth's crust. The average concentration of boron in soil is from 10 to 20 mg/L, and in seawater ranges between 0.5 mg/L to 9.6 mg/L. The boron content of other waters (such as wastewater, fresh waters) is determined by the industry and the waste streams. Turkey has the biggest boron reserves in the world and the world's boron sources are given in Figure 2 below. Boron is present in aqueous solutions as boric acid and borates, depending on pH and the concentration of boron species. At 25 °C, with a pKa value of 9.2, boric acid is a weak acid and having the equation (1) below.

$$B(OH)_3 + OH^- \rightarrow B(OH)_4^- \tag{1}$$
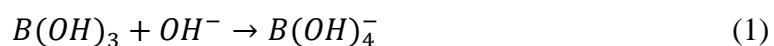
At low pH values the dominant form of boron species is boric acid whereas at high pH values, borate ions dominate as shown in Figure 3 below, The concentration of boron

species also dictate the borate ion species, for example at concentrations higher than 216 mg/L, polynuclear boron species of $B_2(OH)_6^{2-}$, $B_3O_3(OH)_4^{-}$, $B_4O_5(OH)_4^{2-}$ form, at lower concentrations $B(OH)_3$ and $B(OH)_4^{-}$ form. In the concentrations below 290 mg/L, the polynuclear species can be neglected [9], [19].
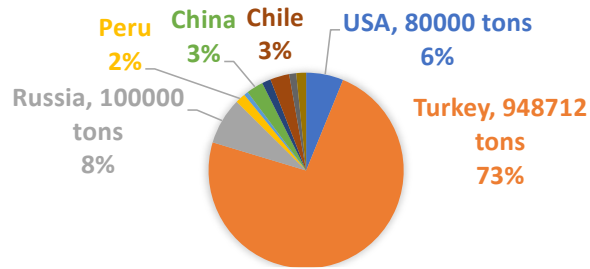
Figure 2. Distribution of boron sources in the world (Source: etimaden.gov.tr)
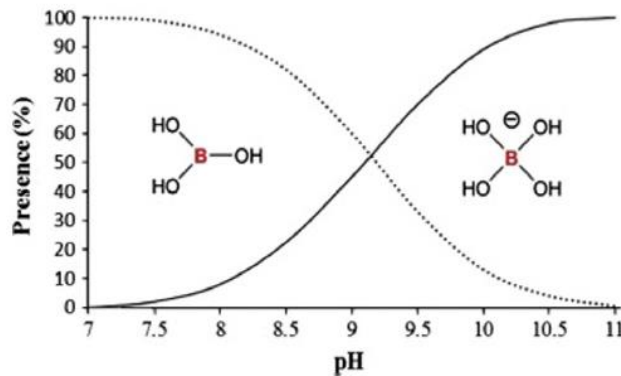
Figure 3. Boric acid and borate ions at various pH values [9]

While boron is an essential micronutrient and a useful component for various industries, it becomes toxic after the boron amount exceeds the required amount and the safe band of boron content in aqueous solutions is very narrow, for example, sunflower plant needs 0.5 ppm boron while 1 ppm is toxic for the plant [19].

Boron toxicity is also affiliated with exposure amount, frequency, and time. Fresh water shortages around the world, combined with the chemistry of the geography around the soil, attains a need to desalinate irrigation and fresh water for appropriate boron content.

5

Boron in water sources can be reduced significantly with thermal desalination technology, but the energy cost of the process it is not favored, methods like reverse osmosis allow for an environmentally friendly way to remove boron, with the shortcoming of lower efficiency due to the chemistry of boron. For example, in seawater boron is present largely uncharged and in boric acid form, which can diffuse through the reverse osmosis membranes and make the separation difficult.

2.3. Boron Removal Methods

To remove boron from aqueous solutions, various methods have been employed such as reverse osmosis, adsorption, ion exchange, dialysis, electrocoagulation along with chemical coagulation and the hybrid processes of these methods. Methods such as crystallization and evaporation are mostly employed in boric acid production, rather than boron removal.

Among those methods, adsorption is seen as the most promising method while removing boron from aqueous solutions of low concentrations such as seawater, saline waters with reverse osmosis membranes coming second, as their efficiencies were compared in Table 1 below. Ease of the operation in adsorption makes it feasible. And in adsorption, various sorbents such as fly ash, activated carbon, natural materials, zeolites, oxides, nanoparticles and selective resins are used [9], [20].

Table 1. Commonly used boron removal methods

Method	Boron Removal (%)	Remarks	Reference
RO Membrane	40-60% 95%*	Boric acid removal Borate ion removal	Prats et al. (2000)
SWRO Membrane	70-90%	Very high pressures (~55 bars)	Koseoglu et al. (2008)
Adsorption	>99% 93-94%	Selective resins Fly Ash	Guan et al. (2016)

2.4. Commonly Used Sorbents in Boron Removal

For the removal of boron, various sorbents are used such as fly ash, clays, natural materials, activated carbons, oxides, zeolites, nanoparticles, and selective resins. Chelating resins is one of the most effective materials for the boron removal [9]. Also, it is important to use an environmentally friendly adsorbent with properties such as rapid adsorption kinetics, and reusability. In this part, boron adsorbents in literature were investigated and proposed adsorbent synthesis route was given.

2.4.1. Chelating Resins

Chelating resins usually have microporous polystyrene matrix, attached to functional hydroxyl groups that are called vis-diols. As seen in **Figure 4** below, ligands of the resin contain three or more hydroxy groups that have an affinity for boron while being non-reactive for other metals present in the solution. Therefore, they enable selective sorption of the boron to the material. One of the most studied and used resins are synthesized with N-methyl-D-glucamine (NMDG) of copolymer of styrene and divinylbenzene [20].
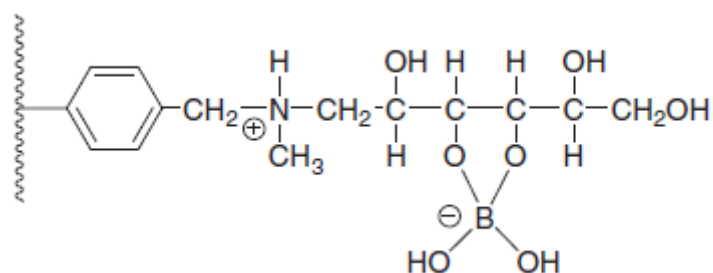
Figure 4. Chelating resin compexing borate with NMDG group [9]

While studies of synthesizing boron selective resins of different functional groups than NMDG gained interest lately, most of the commercially used resins for boron removal such as, Amberlite IRS 743, BSR1, Diaion CRB03, Diaion CRB05, are prepared with NMDG group, and can present removal efficiency of 93-98% boron removal [20]. Commonly used resins for boron removal were listed in Table 2 below.

Table 2. Commonly used adsorbents for boron removal [4]

Polymer Support	Functional Group	Mode	Capability (mg/g)	Isotherm models and Adsorption Kinetics
GMA-PE	NMDG	Batch	14.5	-
GMA-PE-PP	NMDG	Column	23.8	Freundlich
Silica-polyallylamine Composites	NMDG	Batch	16.8	Chemical rxn model
PVA	Glucose	Batch	26.7	Freundlich
PAA	Glucose	Batch	32.9	Freundlich
GMA-dehydrochlorinated PVC	Iminodipropylene glycol	Batch	27.0	Pseudo second order
Amberlite IRA743	-	Batch	5.41	Pseudo second order

2.4.2. Activated Carbon

Activated carbon as an adsorbent, is used in various waste treatment industries because of the high surface area of the material. Because of the lower surface specific active groups for boron removal, causing low adsorption selectivity, is not used widely. Modified versions of active carbons such as curcumin-impregnated AC can achieve nearly 50% more adsorption capacity of boron than bare AC [9], [21].

2.4.3. Industrial Waste Materials and Fly Ash

Various waste materials such as aluminum-based water treatment residuals, waste concrete, palm oil mill boiler, and fly ash that contains silica, can be used for boron removal as well as for metal adsorption. For example, it was stated that, with aluminum-based water treatment residuals, adsorption capacities up to 0.980 mg boron /g adsorbent can be achieved [22]. As a promising candidate, concrete particles that are calcined at 175 °C, could remove 99.8% of boron present [9].

2.4.4. Natural Materials

Natural materials such as natural minerals like muds and clays, and plant residuals like seeds, natural polymers can be used for boron removal. Main advantage for these materials is the availability and low cost with the down come of pretreatment of the natural material. Generally chemical modification is needed for the preparation of the adsorbent. Also, organic materials were showing better boron removal performance then minerals [9].

The studies on the bentonite, kaolinite, zeolite, calcite materials showed that chemical modification using $FeCl_3$ was enhancing boron adsorption process. The influence of $FeCl_3$ affects the zero-point charge of the sorbent and results in negative charge formation on the surface, therefore attracts H_3BO_3.

Among the natural materials, some natural polymers like chitosan, and cellulose gained interest due to amino and hydroxyl groups already present in their structure to help boron removal in the process and for their abundance in nature. It was shown that cellulose can form a stable platform for NMDG moieties [23]. Also, the adsorption kinetics of the natural materials were explained with pseudo-second-order rate which indicates a chemical interaction between boron and the natural adsorbents. Natural materials can be used to take part in other methods for different duties. In Table 3 below, various natural materials were listed for the candidates for boron removal.

Table 3. Natural materials for boron removal [9]

Adsorbent	Modification	Mode	Conditions	Capability (mg/g)	Isotherm Models	Kinetics
Waste Calcite	$FeCl_3$	Batch	pH 9	1.6	Langmuir	-
Rice Residues	-		pH 8	9.26	Freundlich	-
Sepiolite	HCl	Batch	pH 10	178.57	Langmuir	Thomas & Yoon and Nelson
Vermiculite	H_2O_2, Thermal shock, Ultrasound	Batch	pH 9.26	1.62	Freundlich	-
Pomegranate seed powder	PVA	Column	pH 8	38.5	Langmuir	Modified-dose–response model
Chitosan	-	Batch	pH 8	3.9	Freundlich	Pseudo-2nd
Calcium alginate gel	-	Batch	pH 9-10	94	Langmuir	Pseudo-2nd

2.4.5. Oxides and Hydroxides

With high adsorption capacity of heavy metal ions, oxides, and hydroxides are used in the industry. And among those oxides, alumina is the most studied oxide in boron removal. The maximum boron adsorption efficiency of alumina was found to be 40% with activated alumina in 5 mg/L boron solution, reaching a 65% adsorption efficiency with 5 g adsorbent in 50 mg/L boron solution. The pH value of the solution is very important in this case too.

Hydroxides such as calcium hydroxide, form complexes with the borate ions, are also studied for the boron removal processes and the removal rate of boron goes up to 77% [9].

2.4.6. Inorganic Sorbents

Materials such as mesoporous silica, zeolites and nanoparticles are studied recently for boron adsorbent synthesis recently. For example, in Figure 5. below, structure of mesoporous silica with high surface area utilized to be a hybrid sorbent for boron removal processes was shown and can adsorb boron better than commercial Amberlite IRA 743 material with a capacity of 45% boron removal [9]. NMDG was used as the functionalizing agent for boron removal in these types of materials mostly.
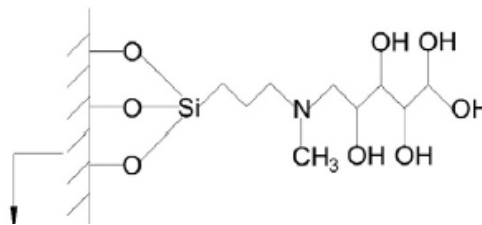
Figure 5. Mesoporous silica modified with NMDG

Also, zeolites were utilized as boron sorbents and can go up to 75% boron adsorption capacity. Other types of inorganic sorbents include magnetic nanoparticles, Fe impregnated nanoparticles, and carbon nanotubes.

2.4.7. Complexing Membranes

Membranes with complexing polymers grafted onto membrane surfaces studied for boron adsorption. These types of membranes can be used in normal pressure as comparison of reverse osmosis membranes that need higher pressures, thus reducing the energy need of the process. Also, complexing membranes show good stability under high saline conditions. For example, regenerated cellulose membranes which grafted with poly-GMA and functionalized with NMDG can adsorb up to 8.11 mg boron per g of

sorbent at neutral pH, which was comparable with commercial products for boron removal [9].

2.5. Proposed Adsorbent Synthesis Route

After examining the adsorbents in literature, this study focused on using a renewable support material for the proposed absorbent to host NMDG functional group that is very boron selective. For this reason, as an abundant material that can be used as a support, cellulose was chosen.

2.5.1. Cellulose Sources in Turkey

As a potential, not utilized cellulose source, Turkey is rich in hazelnut shells in the Black Sea region. In the Mediterranean region, olive trees are the oldest crops and are cultivated over 11 million ha, with the world's biggest olive production coming from Spain, Italy, Greece, and Turkey, respectively, as shown in Figure below [24]. Pruning a hectare of olive trees generates nearly 3 tons of olive pruning debris, resulting in a total of 3.3×10^7 tons worldwide each year and the pruning debris is mostly used for energetic purposes. With the average composition of 33.2 % cellulose, 20.38 % hemicellulose and rest lignin [24], olive pruning waste can be utilized as a renewable cellulose source to produce boron selective biosorbents. Previously, olive tree-based adsorbents are utilized for removal of chemicals such as lithium [25], chromium [26] and lead [27] but for boron removal, olive tree waste are not utilized as a boron selective adsorbent. Therefore, there is a potential for the valorization of olive tree pruning waste as a functionalized biosorbent for boron removal by modifying their surface to achieve high boron removal performance. Hence, in this study, olive tree pruning waste was chosen as the cellulose source to synthesize a novel adsorbent.
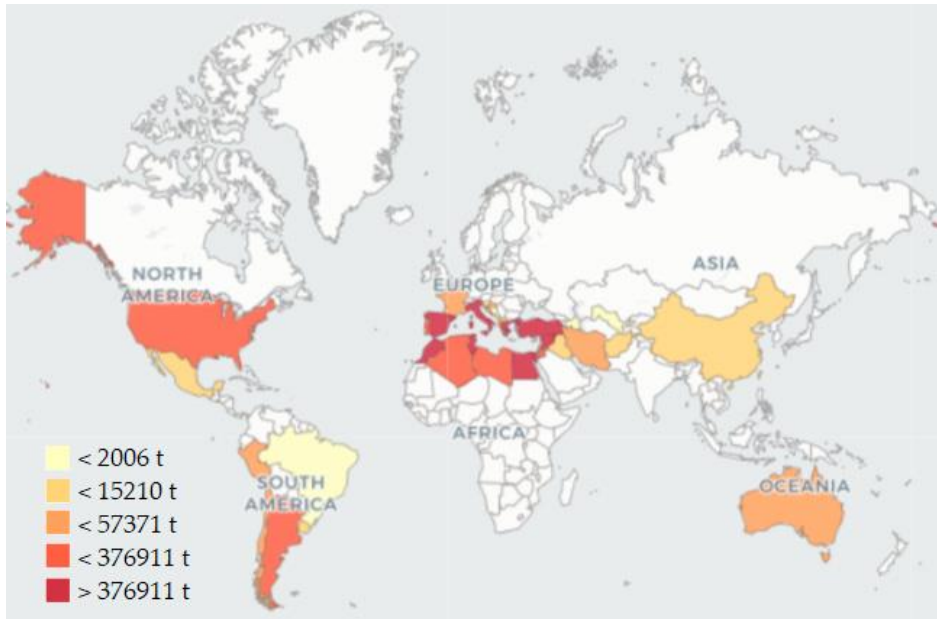
Figure 6. Olive production in the world[24]

CHAPTER 3

METHODOLOGY

3.1. Materials

Olive tree pruning waste (OPW) was gathered from Izmir Institute of Technology campus area. Before utilizing it in the adsorbent synthesis, OPW was thoroughly washed using deionized water, and then crushed into a particle size of 300-500 µm after it was dried overnight in an oven. Glycidyl methacrylate (97%), benzoyl peroxide (75%) and n-methyl-d-glucamine (99%) were supplied from Acros Organics, Belgium. Cellulose microspheres, Boric acid (99.5%), sodium hydroxide and acetone (99.8%), were purchased from Merck, Germany. Geothermal water was supplied from Balçova Geothermal A.Ş (Izmir, Turkey).

Chemicals used in this study were given in Table 4 below.

Table 4. List of chemicals

Chemicals	Chemical formula	Manufacturer
Sodium hydroxide,	NaOH	Merck, Germany
Hydrochloric Acid (37%)	HCl	Merck, Germany
Olive branches	NA	--
Glycidyl methacrylate (97%)	$C_7H_{10}O_3$	Acros Organics, Belgium
N-Methyl-D-glucamine (99%)	$C_7H_{17}NO_5$	Acros Organics, Belgium
Boric Acid	H_3BO_3	Merck, Germany
Geothermal Water	--	Balçova Geothermal A.Ş.

3.2. Adsorbent Synthesis

In the adsorbent synthesis part, the procedure was first applied to pristine cellulose to confirm the procedure. After determining the successful synthesis of the adsorbent from pristine cellulose with characterization results and preliminary adsorption results, the exact procedure was applied to real biomass denoted as OPW. In this section, the procedure was written as if it is only applied for the OPW to not repeat the whole procedure again for the ease of reading.

3.2.1. Alkali Pretreatment

In order to remove hemicellulose and lignin present in the lignocellulosic structure of OPW and expose the hydroxyl groups for GMA grafting, following alkali treatment was applied [25]. 10 g of 250-500 µm particle OPW was reacted with 100 mL of 10 M NaOH solution at 25 °C. Resulting mixture was mixed with 10 M HCl (100 mL) to precipitate cellulose dominant OPW dissolved in the media. After the precipitation, resulting mixture was thoroughly washed with distilled water until pH of 7 reached, then filtered and dried at 60°C overnight. Remaining solid was collected as alkali treated OPW (AT-OPW). This step was not applied for the synthesis of the pristine cellulose-based adsorbent.

3.2.2. GMA Grafting

There are several techniques for grafting cellulose such as radiation [28] and chemical grafting, and other methods that generate radicals for polymerization [10]. In this case, grafting of GMA onto cellulose was achieved through utilization of benzoyl peroxide (BPO) as the chemical initiator for the reaction. GMA grafted cellulose was synthesized using pristine cellulose and AT-OPW in the biomass case, as the base

material, similar to a synthesis route explained for pristine cellulose in previous works [16]. A mixture of AT-OPW (3 g), GMA (8.2 g) and BPO (0.4 g) were prepared using 45 mL of deionized water + acetone mixture (2:1 volume ratio) and put into a 3-neck flask. Nitrogen gas was used to purge the reaction mixture, then, the flask was sealed, and GMA grafting reaction took place at 65 °C for 2 hours as illustrated in Figure 7a.

After the reaction, the resulting mixture was filtered and washed with deionized water and acetone to remove unreacted agents. Also, to remove polyglycidyl methacrylate that may have been produced in the reaction, 10 cycles of Soxhlet extraction using acetone were performed to remove polyglycidyl methacrylate homopolymer [29], [30]. The obtained material was dried at 50 °C overnight, then ground in a mortar then collected as GMA-grafted OPW (G-OPW).
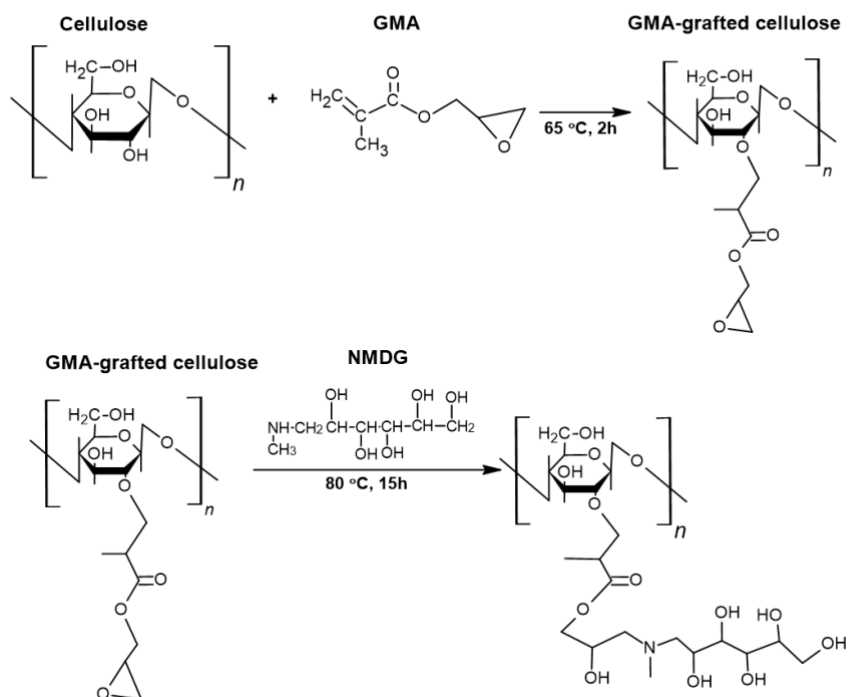
Figure 7. Scheme for (a) GMA grafting and (b) NMDG attachment

3.2.3. NMDG Attachment

To attach NMDG functional group via the ring opening reaction of GMA, a mixture of G-OPW (3 g) and NMDG (16.1 g) [23] were prepared in deionized water (64 mL) for the reaction illustrated in Figure 7. The resulting mixture was held at 80°C, 750 rpm to carry out the reaction for 15 hours. At the end of reaction, remaining solids were filtered and washed to eliminate the NMDG moieties that are highly water soluble with deionized water. Solid residue was dried at 50°C and collected as final cellulose-based adsorbent (N-OPW).

3.3. Adsorbent Characterization

The surface morphologies of OPW, AT-OPW, G-OPW and N-OPW containing NMDG functional groups were investigated with SEM (250 FEG, FEI QUANTA) analysis. The changes occurred in the bond structures of OPW, G-OPW, AT-OPW and N-OPW were observed by recording IR spectra in the range of 4000-400 cm^{-1} using a Perkin Elmer UATR-FT-IR device (4 cm^{-1} resolution, 20 scans per sample). To determine the thermal stability of OPW, AT-OPW, G-OPW and N-OPW, thermogravimetric analysis was done in nitrogen environment with a heating rate of 10 °C/min between 30 and 800 °C, with Shimadzu TGA-51 equipment. Elemental compositions of the synthesized adsorbents were found using LECO 932 CHNS elemental analyzer (Leco-932, USA).

3.4. Batch Adsorption Studies

Adsorption performance of synthesized N-OPW were studied by performing batch adsorption experiments using 10 ppm boron model solution and geothermal water from Balçova Geothermal. Effect of adsorbent dosage, pH, temperature, and initial boron

concentration were investigated. Varying boron model solution concentrations (10-100 ppm) were used to investigate effect of concentration. The experiments were carried out in closed plastic flasks of 50 mL and in a shaking incubator at 180 rpm for 24 hours with two replicates. Also, the conditions of preliminary adsorption experiments of the pristine cellulose-based adsorbent were mentioned in relevant parts of this section.

3.4.1. Effect of Adsorbent Dosage

In order to determine the required amount of adsorbent for removal of boron from 10 ppm boron model solution, various adsorbent amounts (0.05-0.4 g) were used in 50 mL boron model solution in batch adsorption studies. Also, optimum adsorbent amount for boron removal from geothermal water were determined in same manner.

3.4.2. Effect of pH

In order to determine the optimum pH for removal of boron, a study with varying pH value between 2 and 12 was performed. Adsorbent amount and boron model solution were same for each pH value. The pH adjustment of adsorption media was done using HCl and NaOH solutions.

To determine the pH of zero-point charge (pH_{PZC}), where the net charge of N-OPW surface is zero, the following pH drift procedure was applied [31], [32]. 0.10 g of N-OPW was added to 100 mL flasks containing 50 mL NaCl solution (0.01 mol L^{-1}) with an adjusted initial pH between 2 to 12. The pH was adjusted using NaOH or HCl solution (0.5 mol L^{-1}), and the flasks were purged with nitrogen gas for 2 minutes to eliminate CO_2 effect on the pH change. The flasks were then sealed and shaken in a water bath shaker at 180 rpm, 25 °C for 24 hours. The final pH values of each flask were measured and plotted against the initial pH to obtain ΔpH. The pH_{PZC} of N-OPW was determined as the pH at which the curve intersected the line $\Delta pH = 0$.

3.4.3. Effect of Initial Concentration and Temperature

To check the effect of temperature on adsorption process and determine the adsorption isotherms, a series of batch adsorption studies with various initial boron concentrations (10-25-50-75-100 ppm) and temperature (25-35-45 °C) were performed.

3.4.4. Boron Concentration Measurement

At the end of experiments, remaining liquid product was analyzed via ICP-OES (Agilent Technologies, 5110) to determine boron removal. Following equations were used to calculate the adsorption capacity (q) and boron removal (r):

$$q = V \frac{(C_0 - C_e)}{m} \qquad (2)$$

$$r = \frac{C_0 - C_e}{C_0} x100 \qquad (3)$$

3.5. Adsorption Kinetics

To understand the kinetics of the synthesized adsorbents, a series of kinetic studies were carried out in boron solution, using optimum adsorbent amount. The least-squares regression approach [33] was used to fit pseudo-first-order [34] and pseudo-second-order [35] kinetic models as shown in Eq. 5 and Eq. 6 to the experimental data, respectively.

$$q_t = q_e(1 - e^{-k_1 t}) \qquad (4)$$

$$q_t = \frac{k_2 q_e^2 t}{1 + k_2 q_e t} \qquad (5)$$

where q_t (mg/g) is the quantity of boron adsorbed at a specific time while t is time (min), and q_e (mg/g) is the amount of boron adsorbed at equilibrium, and k's are the rate

constants for the models. To find the best fitting model, obtained R^2 values were compared.

3.6. Adsorption Isotherms

To determine the highest adsorption capacity and comprehend how boron species adsorb to the synthesized adsorbents, pristine cellulose based adsorbent and OPW based adsorbent were equilibrated with different boron concentrations (10 to 100 mg/L), and adsorption isotherm models were applied to experimental data. Using the experimental data from the adsorption results of various boron concentrations, adsorption isotherms were modeled with following Langmuir [36] (Eq. 6) and Freundlich [37] (Eq. 7) equations using least-squares regression method:

$$q_e = q_{max}\left(\frac{K_L C_e}{1+K_L C_e}\right) \qquad (6)$$

$$q_e = K_F C_e^{\frac{1}{n}} \qquad (7)$$

where q_e (mg/g) is the amount of boron adsorbed at equilibrium, q_{max} is maximum amount of boron adsorbed (mg/g), K_L is Langmuir isotherm constant (L/mg), K_F and n are Freundlich isotherm constants [28].

CHAPTER 4

MATERIALS AND METHODS

4.1. Characterization Results

In the following results and discussion section, the results of both pristine cellulose and olive pruning waste (OPW) based adsorbents were given simultaneously in their relevant places for comparison. The pruning waste-based adsorbent was denoted as OPW and pristine cellulose-based adsorbent was denoted as pristine cellulose based adsorbent.

4.1.1. GMA Grafting Percent and NMDG Density

The pristine cellulose and olive pruning waste was grafted with GMA to attach boron selective NMDG groups to the resulting epoxy rings on the grafted cellulose. GMA was grafted onto the surface of cellulose with benzoyl peroxide as the initiator for the reaction. The resulting adsorbents were given in Figure 8.

Figure 8. GMA grafted cellulose (a) right after Soxhlet (b) after drying GMA grafted
OPW (c) right after Soxhlet (d) after drying

Grafting efficiency and percent grafting were calculated from the following equations given below:

$$P_g = \frac{Weight\ of\ GMA\ grafted\ cellulose - Weight\ of\ cellulose}{Weight\ of\ cellulose} \times 100 \qquad (8)$$

$$\%G = \frac{Weight\ of\ GMA\ grafted\ cellulose - Weight\ of\ cellulose}{Weight\ of\ GMA\ introduced} \times 100 \qquad (9)$$

Using pristine cellulose, P_g was found as 174.6% and %G was 63%. For OPW, P_g and %G were found as 184.6% and 67.5%, respectively. Comparing the results with the literature, higher grafting efficiency and percent grafting were achieved for both the cellulose and OPW [30].

After the NMDG binding reaction, resulting adsorbents were given in Figure 9.

Figure 9. NMDG attached adsorbent (a) pristine cellulose (b) N-OPW

The density of NMDG groups present on the adsorbent can be calculated from the weight of the final adsorbent, and calculated from the following equation:

$$D_N \left(\frac{mmol}{g}\right) = \frac{\frac{W_f - W_g}{W_f}}{MW} * 1000 \qquad (10)$$

where W_f is weight of the final adsorbent, W_g is weight of the GMA grafted adsorbent and MW=195.2 g/mol for NMDG. D_N was found as 2.1 mmol/g for the pristine cellulose based adsorbent and 1.97 mmol/g for the OPW based adsorbent. Since the OPW-based

adsorbent contains more GMA on the surface than the pristine cellulose (higher %G), lower NMDG density was expected on the OPW surface. The NMDG density of the synthesized adsorbents was similar to other NMDG type adsorbents reported in the literature that were prepared with various solvents (i.e., water, dioxane) [1], [18], [38].

Also, after G-OPW was modified with NMDG functional group, the density of NMDG moieties on the N-OPW surface was determined from elemental analysis of the samples. Elemental analysis results of the synthesized adsorbents were given in Table 5. Since the only N containing reagent was NMDG in the synthesis step, the NMDG density of the adsorbent was calculated as 2.07 mmol/g for N-OPW. Which is very similar (%5 error) to the value calculated from weight differences before. The elemental analysis results suggested that NMDG was successfully introduced to GMA grafted surfaces.

Table 5. Elemental composition of samples

Sample	C%	H%	N%	O%
OPW	45.20	6.63	0.65	47.53
AT-OPW	43.71	8.31	1.53	46.45
G-OPW	57.02	9.42	0.65	32.91
N-OPW	49.72	10.68	3.30	36.31

4.1.2. FT-IR Analysis

When FT-IR spectra of pristine cellulose and GMA grafted pristine cellulose are compared in Figure 10, due to the GMA introduction into the structure of cellulose, the characteristic peak of C=O related to GMA formed with the addition of a high amount of carboxyl groups at 1722 cm^{-1} and the peaks attributed to the epoxy rings at 845 cm^{-1}, 757-788 cm^{-1} and 905 cm^{-1} formed, and the results are in line with literature [4], [29], [38]. Also, the addition of GMA to the -OH groups of cellulose as proposed in the reaction scheme given in Figure 7, resulted in decrease of -OH peaks at 3320 cm^{-1} and suggesting successful binding of GMA to AT-OPW [1]. As a result of NMDG binding to grafted cellulose, previously disappeared -OH peaks at 3320 cm^{-1} reappeared due to the addition

of -OH groups present in the NMDG structure. The peaks belonging to amide 1 and amide 2 groups were observed at 1645 and 1544 cm^{-1}, respectively[1], [39]. Since the only nitrogen source was NMDG group, the results also proved that functional group binding was successfully accomplished. In addition, the peaks belonging to the epoxy groups that were present in grafted cellulose disappeared or decreased with the binding of the NMDG functional group, thus suggesting the NMDG groups were attached to epoxy rings as shown in the reaction scheme and this phenomenon is in line with literature [11], [29], [30]. The results when OPW was used as a starting material for the adsorbent synthesis were given in Figure 11. Nearly identical results were obtained, since OPW was real biomass, there were some noises in the spectra.
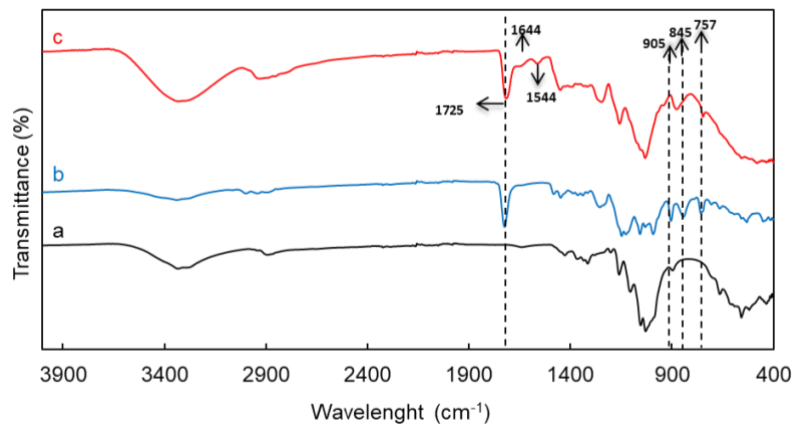
Figure 10. FTIR spectra of (a) pristine cellulose (b) GMA grafted cel. (c) NMDG attached cellulose
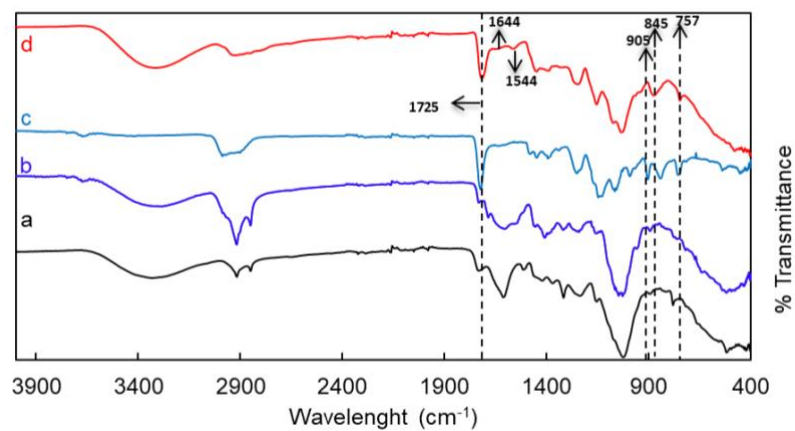
Figure 11. FTIR spectra of (a) OPW (b) AT-OPW (c) G-OPW (d) N-OPW

4.1.3. SEM Analysis

The morphological structure of the GMA grafted pristine cellulose surface became rougher than raw cellulose due to the addition of GMA into its structure as shown in Figure 12 below. It is clearly seen that NMDG functionalized cellulose turns into a more crystalline, smooth structure while raw cellulose and grafted cellulose have more fibrous structure. Therefore, the surface of the raw cellulose has undergone morphological changes because of grafting with GMA and introduction of NMDG functional groups into its structure.
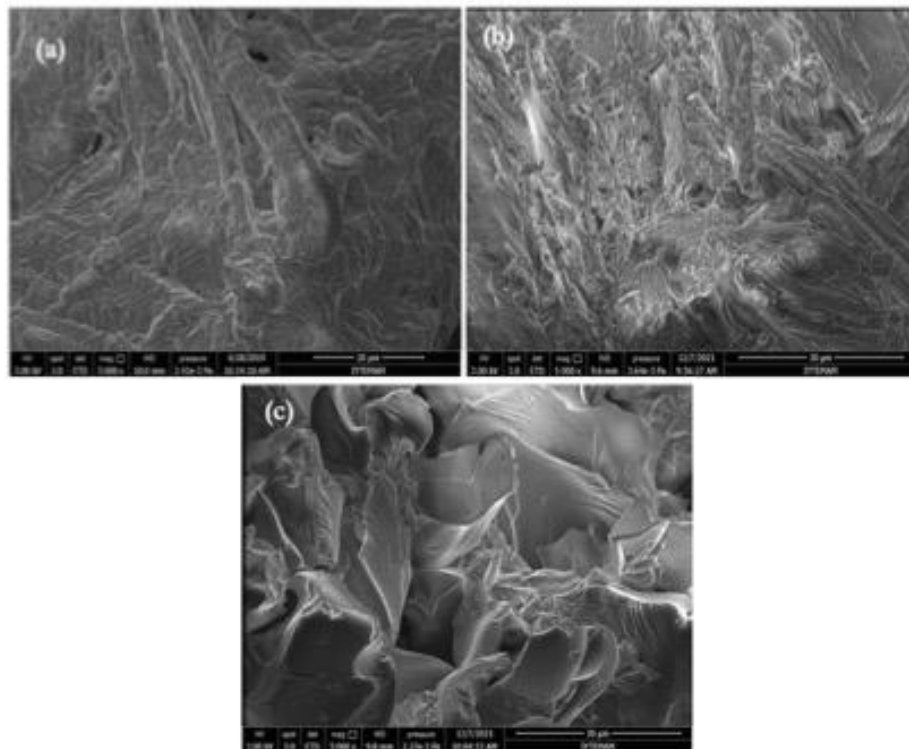
Figure 12. SEM images of (a) Pristine cellulose (b) GMA-grafted (c) NMDG
            attached

The SEM images when OPW was used as a starting material for the adsorbent synthesis were given in Figure 13. Compared to OPW (a), surface of AT-OPW (b) become rougher, exposing more cellulose. After the GMA grafting reaction,

morphological structure of G-OPW (c) surface was coated due to the addition of GMA into its structure. It is clearly seen that N-OPW (d) turns into a more crystalline, smooth structure. Therefore, the surface of OPW, AT-OPW and G-OPW had undergone morphological changes because of alkali treatment and grafting with GMA and introduction of NMDG functional groups into its structure respectively.
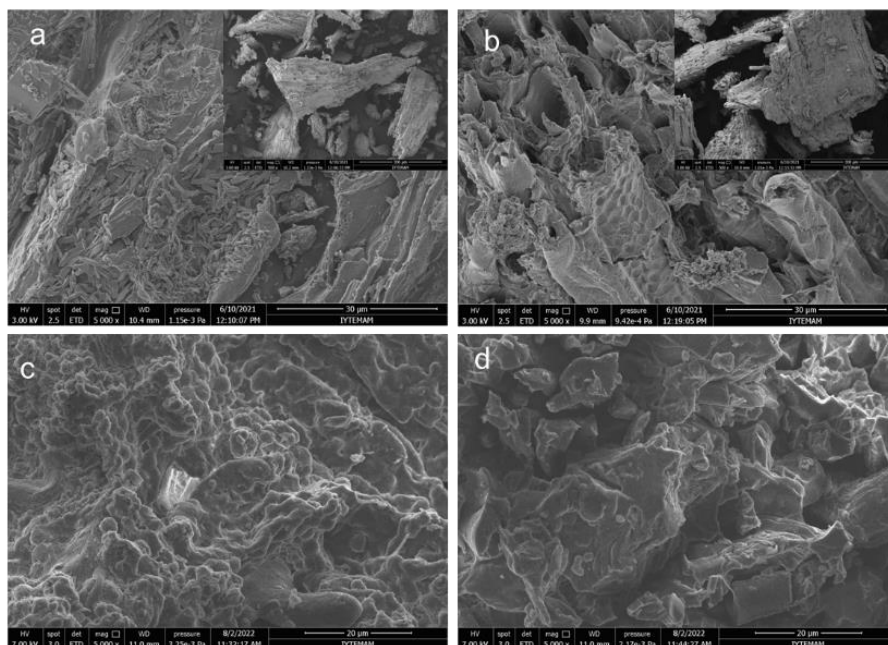
Figure 13. SEM images (5000x) of (a) OPW, (b) AT-OPW, (c) G-OPW,(d) N-OPW

4.1.4. Thermogravimetric Analysis

Thermograms of OPW, AT-OPW, G-OPW and N-OPW were given in Figure 14. Similar thermal characteristics were obtained with the pyrolysis process for OPW, AT-OPW and G-OPW. The water molecules adsorbed on surface as the moisture caused decrease in weight% around 100 °C for all samples [40]. Decomposition of cellulose present in all samples occurred between 300-400 °C as stated in the literature [11]. Moreover, the presence of GMA groups in the G-OPW increased the decomposition temperature compared to AT-OPW, resulting a higher decomposition temperature while N-OPW decomposed at slightly lower temperatures than AT-OPW and G-OPW.

Modification steps changed the decomposition profile for all samples and, N-OPW was thermally stable up to temperatures of about 300 °C, similar to NMDG functionalized cellulose-based adsorbents in the literature [28]. Characterization studies (SEM, TGA, and FT-IR) of cellulose-based adsorbent indicated the successful synthesis of N-OPW adsorbent.
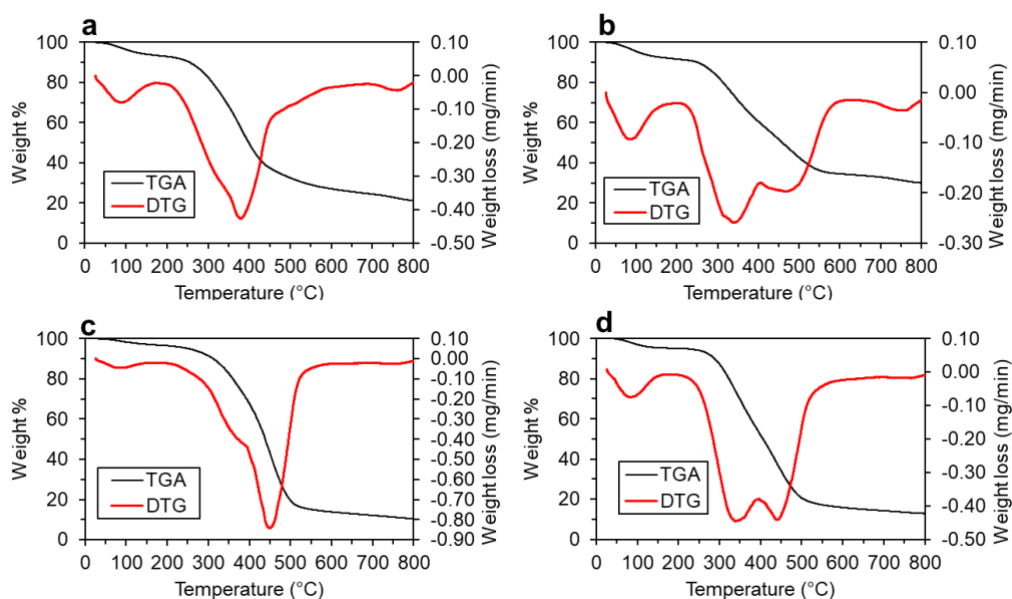
Figure 14. TGA and DTG thermograms of (a) OPW, (b) AT-OPW, (c) G-OPW, and (d) N-OPW

4.2. Batch Adsorption Results

The results of adsorption experiments conducted using OPW based adsorbent (N-OPW) were given in this section. If applicable, preliminary adsorption experiments performed with the pristine cellulose-based adsorbent were also given in relevant parts of this section to compare with the OPW based final adsorbent.

4.2.1. Effect of Adsorbent Dosage and pH

Batch adsorption studies were performed using 10 ppm boron model solution at various pH and adsorbent dosage levels for 24 hours to determine the optimum adsorbent dosage and operating pH to employ in further experiments. The results of pristine cellulose-based adsorbent were given in Figure 15. Almost complete boron removal (99.05%) was observed at 4 g/L adsorbent dosage. Increasing adsorbent dosage further did not increase boron removal significantly. Hence, 4 g/L adsorbent dosage was selected as the optimum for this adsorption conditions. After selecting optimum adsorbent dosage, the effect of pH over boron removal was investigated in the range of pH 2 to 10 for 24 hours using 10 ppm of boron model solution.

As given in Figure 15b, the boron removal did not change with pH significantly, the highest boron removal was observed at pH 10. Cellulose-based adsorbent showed high stability for boron removal in wide pH range.
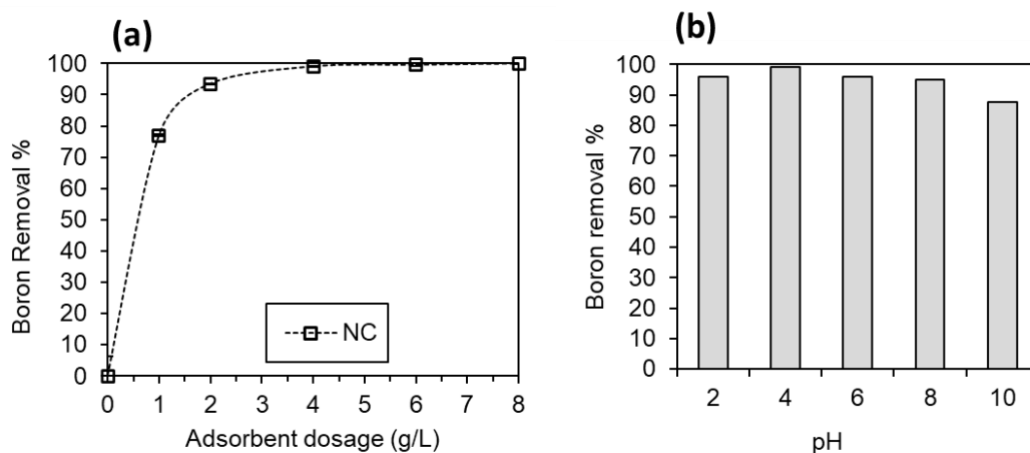
Figure 15. Effect of parameters: (a) Pristine Cel. based adsorbend dosage (C$_0$=10 mg/L, T=25 °C, pH=6, adsorbent dosage=0-8 g/L), (b) Effect of pH on boron removal (C$_0$=10 mg/L, T=25 °C, adsorbent dosage=4 g/L pH=2-10)

Adsorption tests using N-OPW were carried out with 10 mg/L boron solution at different pH and adsorbent dosages to find the best adsorbent dosage and operational pH to use in future experiments and the results were given in Figure 16. At 2 g/L N-OPW dose, nearly full removal of boron (99.21%) was observed. Because no significant

increase was seen, 2 g/L adsorbent dosage was chosen as the best for these adsorption conditions.

N-OPW could achieve same boron removal with half the amount of pristine cellulose-based adsorbent. Since the structure of biomass-based N-OPW was more irregular, this irregular branching phenomenon might lead to more available adsorption sites for boron.

Also, G-OPW did not remove any boron from the solution, suggesting that the boron species cannot attach to GMA. After determining the optimal adsorbent dosage, the influence of pH on boron removal was examined between pH 2 and pH 12. The results of pH effect over boron removal were shown in Figure 16b.
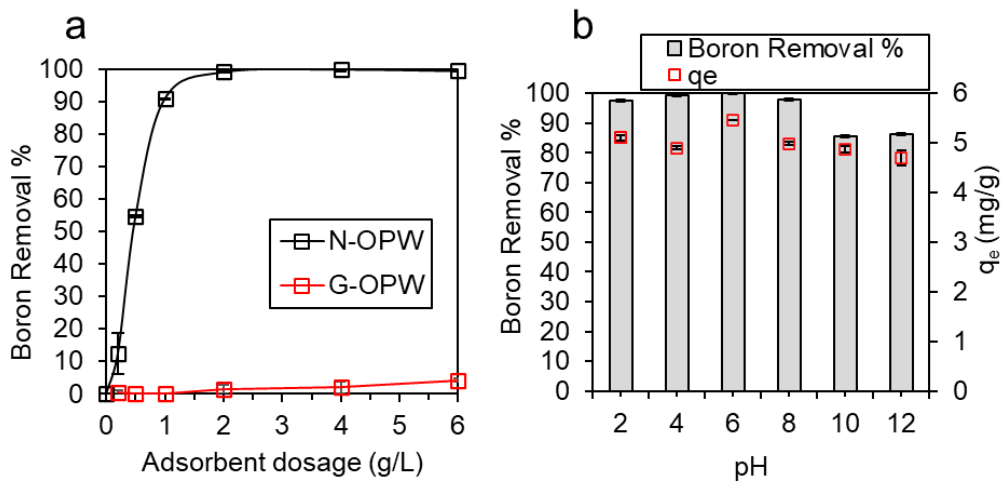
Figure 16. Effect of parameters: (a) N-OPW and G-OPW dosage (C_0=10 mg/L, T=25 °C, pH=6, adsorbent dosage=0-6 g/L), (b) Effect of pH on boron removal and adsorption capacity (C_0=10 mg/L, T=25 °C, adsorbent dosage=2 g/L pH=2-12)

The highest boron removal was obtained at pH 6. Overall, N-OPW functioned well with excellent stability in a wide pH range for the removal of boron. This behavior for NMDG functionalized adsorbents was also reported in the literature. [17], [28], [38], [41]. Therefore, optimum pH value was selected as 6 for further batch adsorption experiments.

To comment more on the adsorption behavior with different pH values, using the pH drift method described before pH_{PZC} value of the N-OPW was found to be 7.6 from the Figure 17 below.
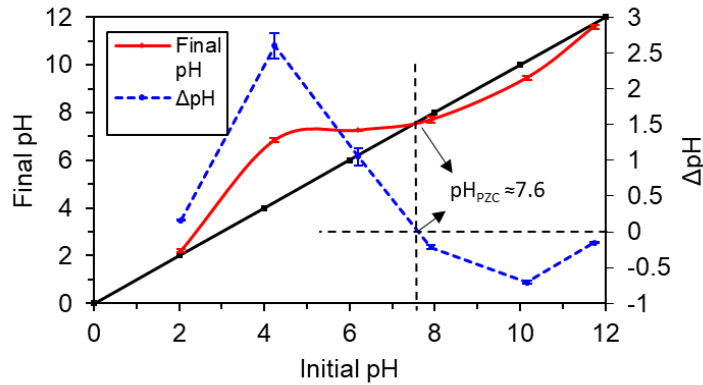
Figure 17. pH of point of zero charge determination

Boron can be present in the solution as boric acid and borate ions. Since borate ions are negatively charged and surface of the N-OPW becomes negatively charged after pH_{PZC}, surface becomes less attractive for anions [13], [42]. As shown in Figure 17, this behavior was observed, when the pH value was increased beyond pH_{PZC}, the adsorbent's capacity to remove boron decreased.

4.2.2. Effect of Initial Concentration and Temperature

The impact of temperature and initial boron concentration on boron removal was studied. To understand this impact, boron solutions with concentrations ranging from 10 to 100 mg/L were tested by contacting them with 2 g/L of adsorbent for 24 hours at 180 rpm and pH 6, while varying the temperature. The results were given in Figure 18.
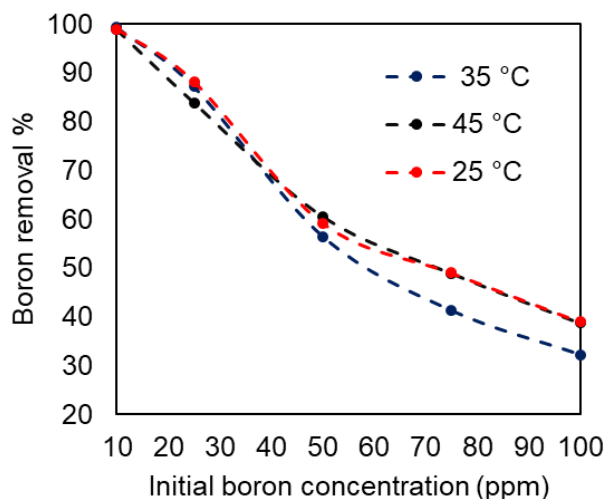
Figure 18. Effect of initial boron concentration and temperature on boron removal
(pH=6, N-OPW dosage=2 g/L)

Highest boron removal was achieved at the lowest temperature with slight deviation at 50 ppm initial boron concentration. At lower concentrations (<50 ppm), boron adsorption seemed to be exothermic, it favored lower temperatures. Normally, temperature increase lowers the attractive forces between the adsorption site and adsorbate and result in a decrease in the physisorption process, since NMDG group selectively captures boron, the temperature increase did not result in this phenomenon for this case. With available adsorption sites, when boron concentration increased, boron adsorption increased as well with temperature. This result can be explained by the coupling of increased diffusion rate with more boron species present in the solution [43].

4.3. Adsorption Kinetics

To understand the kinetic behavior of the pristine cellulose based and OPW based adsorbents, following kinetic studies were carried out.

For pristine cellulose-based adsorbent, a kinetic study in 10 ppm boron model solution using optimum adsorbent amount (4 g/L) at ambient temperature for 24 hours was conducted. The result was given in Figure 19 below.
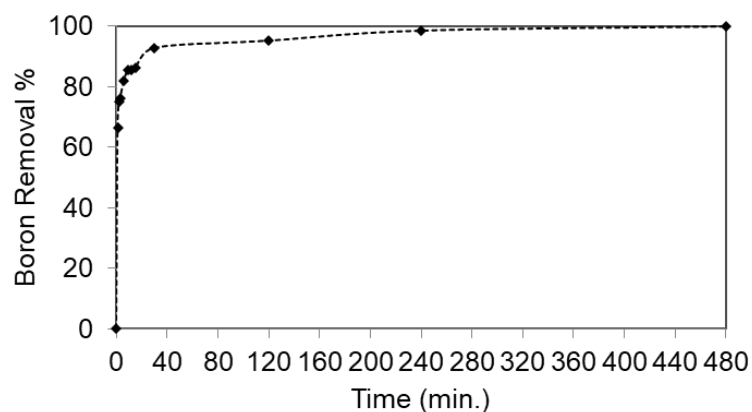
Figure 19. Effect of contact time on Boron removal % (conditions: C_0=10 ppm, T=25 °C, pH=10, adsorbent dosage=4 g/L)

After 4 hours, equilibrium was reached. Boron uptake of the adsorbent in the first minute was found as 66.2%, therefore fast kinetic nature of the adsorbent was observed. Using the least-squares regression approach described in Section 3.5, parameters of the kinetic study were given in Table 6 below. The kinetic mechanism followed pseudo-second-order model kinetics, indicating chemical interactions were involved in the process.

Table 6. Kinetic model parameters of pristine cellulose based adsorbent

Pseudo-first-order model parameters		Pseudo-second-order model parameters	
k_1 (min^{-1})	R^2	k_2 (g.mg^{-1}.min^{-1})	R^2
0.5098	0.7367	0.3274	0.99

In order to comprehend the kinetics of the OPW based adsorbent, a kinetic analysis employing the ideal adsorbent dosage (2 g/L N-OPW) was carried out in a 50 mg/L boron solution and the results of kinetic study were given in Figure 20. Adsorption equilibrium was reached after 2 hours.
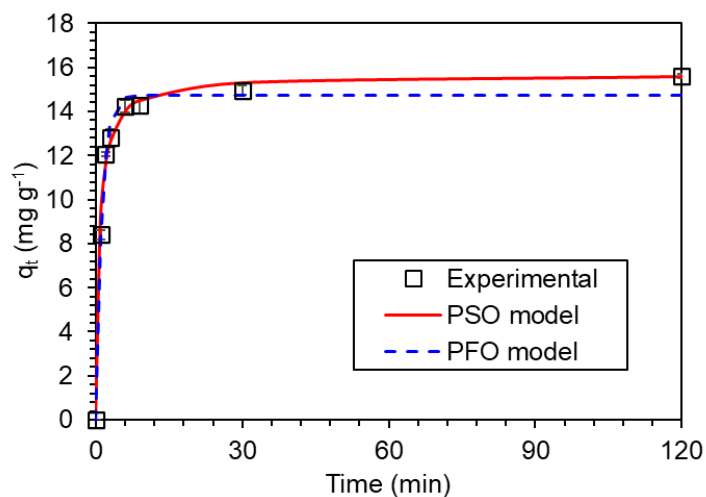
Figure 20. Kinetics of boron adsorption (C_0=50 mg/L, pH=6, N-OPW dosage=2 g/L, T=35 °C)

The results of the kinetic models were summarized in Table 7. Although the R^2 values were very similar, the R^2 value for the pseudo-second-order model was greater than first-order and the predicted q_e value from the model was nearer to the experimental value. Kinetic mechanism of N-OPW followed pseudo-second-order model kinetics too, indicating chemical interactions were involved in the process and similar phenomenon for NMDG modified cellulose-based adsorbents were reported in the literature [17], [28].

Table 7. Kinetic model parameters of N-OPW

Pseudo-first-order model parameters			Pseudo-second-order model parameters			Experimental value
q_e (mg/g)	k_1 (min^{-1})	R^2	q_e(mg/g)	k_2 (g.mg^{-1}.min^{-1})	R^2	$q_{experimental}$
14.73	0.811	0.991	15.66	0.087	0.995	16.56

4.4. Adsorption Isotherms

Langmuir adsorption isotherm relates adsorption to a single-layer and homogenous adsorption on surface whereas Freundlich adsorption isotherm relates the adsorption process to a multilayer, a heterogenous surface adsorption [44].

To determine the highest adsorption capacity and comprehend how boron species adsorb to the adsorbent, 4 g/L pristine cellulose based adsorbent was equilibrated with different boron concentrations (10 to 100 mg/L) and adsorption isotherm models were applied to experimental data and the results were given in Table 8.

Table 8. Isotherm model parameters of pristine cellulose based adsorbent

Langmuir adsorption isotherm parameters				Freundlich adsorption isotherm parameters			
K_L	Q_{max} (mg/g)	R^2 (nonlinear, Qe vs Ce plot)	R^2 (linear, Ce/Qe vs Ce plot)	n	K_F	R^2 (nonlinear, Qe vs Ce plot)	R^2 (linear, lnQe vs lnCe plot)
0.12	19.29	0.910	0.886	3.16	4.01	0.949	0.845

For cellulose-based adsorbent, Freundlich isotherm with a R^2 value of 0.949 fits the experimental data better than Langmuir isotherm. The result suggests a multilayer heterogenous adsorption of boron species onto NMDG functional group [45]. The maximum adsorption capacity of the adsorbent was calculated from Langmuir adsorption isotherm and was found as 19.29 mg/g.

Similarly, 2 g/L N-OPW was equilibrated with different boron concentrations (10 to 100 mg/L) and the results of the adsorption isotherm models were given in Figure 21 and Table 9.
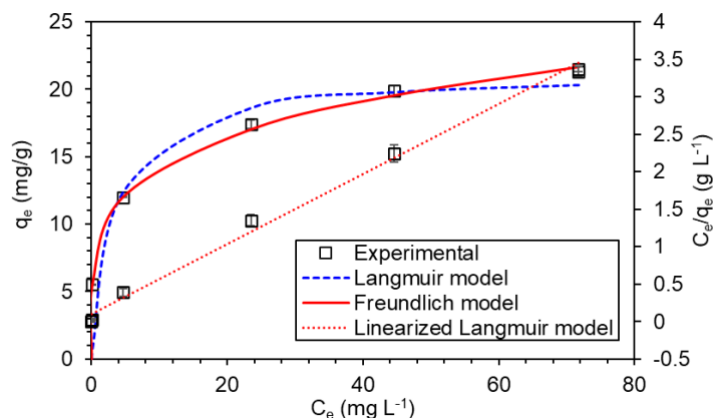
Figure 21. Langmuir and Freundlich adsorption isotherms of N-OPW (C0=10-100 mg/L, pH=6, adsorbent dosage=2 g/L, T=35 °C)

Table 9. Langmuir and Freundlich adsorption isotherm parameters of N-OPW

Langmuir adsorption isotherm parameters				Freundlich adsorption isotherm parameters		
K_L	R^2 (nonlinear, Qe vs Ce plot)	Q_{max} (mg/g)	R^2 (linear, Qe vs Ce plot)	n	K_F	R^2 (nonlinear, Qe vs Ce plot)
0.31	0.849	21.80	0.994	4.64	8.62	0.997

From the results, for N-OPW, Freundlich adsorption isotherm explained the adsorption phenomenon better too, with a R^2 value of 0.997. According to the models, (q_e) was found as 21.80 mg/g from linearized Langmuir model and 21.62 mg/g from nonlinear Freundlich model. The adsorption capacity of N-OPW was higher than commercial resins of Diaion CRB02, CRB05 (13.18 and 17.45 mg/g), and other NMDG-based adsorbents in the literature as given in Table 10 below.

Table 10. Comparison of adsorption capacities of different NMDG functionalized adsorbents

Adsorbent	Adsorption capacity (mg/g)	Reference
Nylon6-VBC-NMDG	13.8	[46]

Table 10. (cont.)

Silica-polyamine-NMDG	16.76	[45]
Diaion CRB02 boron-selective resin (Commercial)	13.18	
Diaion CRB05 boron-selective resin (Commercial)	17.45	
PE-GMA-NMDG	14.5	[18]
Si-NMDG	21.84	[47]
Cellulose-GMA-NMG	4.71	[17]
Pristine cellulose based adsorbent	19.29	This study
N-OPW	21.80	This study

4.5. Thermodynamic Studies

Covering concentrations ranging from 10 to 100 mg/L and temperatures of 25, 35, and 45°, optimal adsorbent quantity of 2 mg/L were employed to determine the thermodynamic parameters, including standard Gibbs free energy change ($\Delta G°$), standard enthalpy change ($\Delta H°$), and standard entropy change ($\Delta S°$). Using the equation (Eq. 9) to calculate the molar free energy change in these experiments, and the KL values from linearized Langmuir isotherm models from the concentration effect experiments.

$$\Delta G° = -RT \ln K_L \qquad (11)$$

where R is (8.314 J/mol.K), T is absolute temperature. Using Van't Hoff equation [48] (Eq. 10), the slope and intercept of $\ln K_L$ versus 1/T plot were utilized to calculate $\Delta H°$ and $\Delta S°$, respectively. Calculated thermodynamic parameters were tabulated in Table 11.

$$\ln K_L = \frac{\Delta S°}{R} - \frac{\Delta H°}{RT} \qquad (12)$$

Table 11. Parameters of boron adsorption thermodynamics onto N-OPW

T (K)	K_L	$\Delta G°$ (kJ/mol)	$\Delta H°$ (kJ/mol)	$\Delta S°$ (kJ/mol)
298.15	0.747	0.72		
308.15	0.569	1.44	-34.14	-0.11
318.15	0.313	3.07		

The negative value of $\Delta H°$ indicated that the boron adsorption was exothermic, and the exothermic nature of the boron adsorption process was observed in the literature with NMDG functionalized adsorbents [17], [45]. The negative $\Delta S°$ was attributed to decrease in the randomness of molecules at the adsorption interface [12].

4.6. Sustainability

The reusability of the N-OPW was investigated under three adsorption/desorption cycles using a mixture of real geothermal water collected from different reinjection wells [49]. Parameters of the geothermal water were given in Table 12.

Table 12. Parameters of geothermal water

Species	Concentration (mg/L)	Species	Concentration (mg/L)
Boron	14 ± 1.7	Sodium	383.6 ± 48.8
Chlorine	196.3 ± 1.5	Magnesium	7.19 ± 1.74
Sulfate	132 ± 13.72	Potassium	32.93 ± 1.64
Fluorine	0.83 ±0.18	Calcium	19.43 ± 6.22
pH	6.5 ± 0.3	Carbonate	616 ± 69.9

2 g/L of N-OPW was contacted with 50 mL geothermal water for 4 hours to adsorb boron species and the mixture was filtered after the adsorption. The used N-OPW was washed with deionized water and equilibrated with 50 mL of 0.5 M HCl solution for 2

hours to desorb boron species. After the desorption, the mixture was filtered and N-OPW was washed with 0.5 M NaOH solution to regenerate and prepare the adsorbent for reuse, the procedure was repeated thrice. The filtrates of adsorption/desorption experiments were analyzed with ICP-OES and adsorption/desorption results were given in Figure 22.
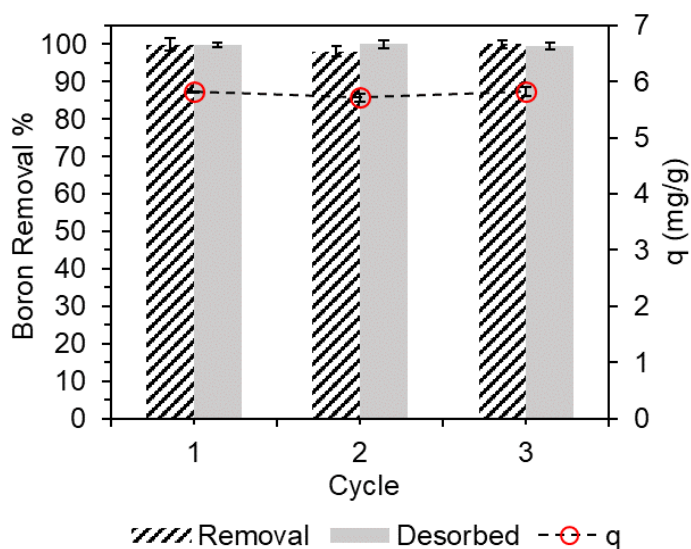
Figure 22. Reusability of N-OPW (C_{geo}=14 mg/L, pH=6, adsorbent dosage=2 g/L, T=35 °C)

Over three cycles of operation, boron attached to N-OPW was desorbed almost completely for all runs (>99%) and boron removal capacity of the adsorbent (q) did not change significantly. The results indicated that N-OPW could be utilized for boron removal from real boron containing water with a reusable and environmentally friendly aspect.

Also, FT-IR spectra of unused, boron loaded and regenerated N-OPW were given in Figure 23 below. As suggested in the boron adsorption mechanism in Figure 7, intensity of -OH groups (3000-3500 cm^{-1}) that were introduced by NMDG addition were decreased when boron species attached, and increased when used adsorbent was regenerated, thus confirming the boron attachment to -OH groups of NMDG.
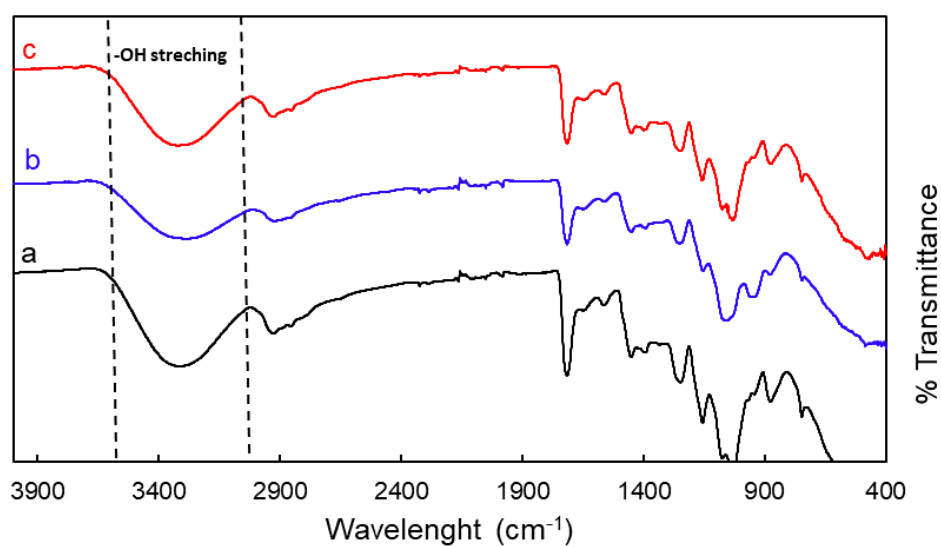
Figure 23. FT-IR spectra of (a) N-OPW, (b) Boron loaded N-OPW, (c) Regenerated N-OPW

Overall, the results indicated a novel, environmentally friendly, reusable adsorbent was synthesized from waste biomass with the GMA grafting and NMDG attachment steps.

CHAPTER 5

CONCLUSION

To remove boron from aqueous solutions, a novel biosorbent was synthesized from olive tree pruning waste (N-OPW) instead of commonly used petroleum based synthetic supports by utilizing alkali treatment, GMA grafting and NMDG attachment steps, respectively. Characterization results (FTIR, TGA and SEM analyses) indicated the successful synthesis of the N-OPW. Adsorption studies revealed that N-OPW had remarkable boron removal capacity as 21.80 mg/g over a wide pH range (2-12). Adsorption studies revealed that the process is exothermic and Freundlich isotherm (R^2=0.99) and pseudo-second-order kinetics (R^2=0.99) gave the best fit for experimental data. Using real geothermal water, a desorption efficiency over 99% for three cycles of operation was achieved and N-OPW showed no significant decrease in boron removal capacity, indicating that a reusable and sustainable adsorbent was synthesized from olive pruning waste and the method potentially can be utilized for other lignocellulosic biomass.

REFERENCES

[1]   T. M. Ting, M. M. Nasef, and K. Hashim, 'Tuning N-methyl-d-glucamine density in a new radiation grafted poly(vinyl benzyl chloride)/nylon-6 fibrous boron-selective adsorbent using the response surface method', RSC Adv, vol. 5, no. 47, pp. 37869–37880, 2015, doi: 10.1039/c5ra00427f.

[2]   A. Mott et al., 'Boron in geothermal energy: Sources, environmental impacts, and management in geothermal fluid', Renewable and Sustainable Energy Reviews, vol. 167, p. 112825, Oct. 2022, doi: 10.1016/J.RSER.2022.112825.

[3]   M. Chen, O. Dollar, K. Shafer-Peltier, S. Randtke, S. Waseem, and E. Peltier, 'Boron removal by electrocoagulation: Removal mechanism, adsorption models and factors influencing removal', Water Res, vol. 170, p. 115362, 2020, doi: 10.1016/j.watres.2019.115362.

[4]   H. Hoshina, J. Chen, H. Amada, and N. Seko, 'Chelating fabrics prepared by an organic solvent-free process for boron removal from water', Polymers (Basel), vol. 13, no. 7, 2021, doi: 10.3390/polym13071163.

[5]   J. Wolska and M. Bryjak, 'Methods for boron removal from aqueous solutions - A review', Desalination, vol. 310, pp. 18–24, 2013, doi: 10.1016/j.desal.2012.08.003.

[6]   M. Bryjak, I. Duraj, and G. Poźniak, 'Colloid-enhanced ultrafiltration in removal of traces amounts of borates from water', Environ Geochem Health, vol. 32, no. 4, pp. 275–277, Apr. 2010, doi: 10.1007/S10653-010-9299-5/FIGURES/2.

[7]   N. Kabay et al., 'Adsorption-membrane filtration (AMF) hybrid process for boron removal from seawater: an overview', Desalination, vol. 223, no. 1–3, pp. 38–48, Mar. 2008, doi: 10.1016/J.DESAL.2007.01.196.

[8]   Ç. Dilek, H. Ö. Özbelge, N. Biçak, and L. Yılmaz, 'Removal of boron from aqueous solutions by continuous polymer-enhanced ultrafiltration with polyvinyl alcohol', http://dx.doi.org/10.1081/SS-120002610, vol. 37, no. 6, pp. 1257–1271, 2002, doi: 10.1081/SS-120002610.

[9]   Z. Guan, J. Lv, P. Bai, and X. Guo, 'Boron removal from aqueous solutions by adsorption - A review', Desalination, vol. 383, pp. 29–37, 2016, doi: 10.1016/j.desal.2015.12.026.

[10]   M. Kumar, P. S. Gehlot, D. Parihar, P. K. Surolia, and G. Prasad, 'Promising grafting strategies on cellulosic backbone through radical polymerization processes – A review', Eur Polym J, vol. 152, no. January, p. 110448, 2021, doi: 10.1016/j.eurpolymj.2021.110448.

[11]   L. Guo, D. Li, H. Lennholm, H. Zhai, and M. Ek, 'Structural and functional modification of cellulose nanofibrils using graft copolymerization with glycidyl

methacrylate by Fe2+–thiourea dioxide–H2O2 redox system', Cellulose, vol. 26, no. 8, pp. 4853–4864, 2019, doi: 10.1007/s10570-019-02411-2.

[12] G. K. Cheruiyot, W. C. Wanyonyi, J. J. Kiplimo, and E. N. Maina, 'Adsorption of toxic crystal violet dye using coffee husks: Equilibrium, kinetics and thermodynamics study', Sci Afr, vol. 5, Sep. 2019, doi: 10.1016/j.sciaf.2019.e00116.

[13] H. Çelebi, I. Şimşek, T. Bahadir, and Tulun, 'Use of banana peel for the removal of boron from aqueous solutions in the batch adsorption system', International Journal of Environmental Science and Technology, vol. 20, no. 1, pp. 161–176, 2023, doi: 10.1007/s13762-022-04566-1.

[14] T. E. Köse, H. Demiral, and N. Öztürk, 'Adsorption of boron from aqueous solutions using activated carbon prepared from olive bagasse', Desalination Water Treat, vol. 29, no. 1–3, pp. 110–118, 2011.

[15] G. N. Manjunatha Reddy, J. A. Gerbec, F. Shimizu, and B. F. Chmelka, 'Nanoscale Surface Compositions and Structures Influence Boron Adsorption Properties of Anion Exchange Resins', Langmuir, vol. 35, no. 48, pp. 15661–15673, 2019, doi: 10.1021/acs.langmuir.9b02042.

[16] B. F. Altınbaş, C. Orak, H. E. Ökten, and A. Yüksel, 'Novel Hybrid Adsorption-Electrodialysis (AdED) System for Removal of Boron from Geothermal Brine', ACS Omega, vol. 7, no. 49, pp. 45422–45431, Dec. 2022, doi: 10.1021/acsomega.2c06046.

[17] A. G. Yetgin, O. A. Dündar, E. Çakmakçı, and Ö. Arar, 'Removal of boron from aqueous solution by modified cellulose', Biomass Conversion and Biorefinery, 2022, doi: 10.1007/s13399-021-02133-1.

[18] T. M. Ting, H. Hoshina, N. Seko, and M. Tamada, 'Removal of boron by boron-selective adsorbent prepared using radiation induced grafting technique', Desalination Water Treat, vol. 51, no. 13–15, pp. 2602–2608, 2013, doi: 10.1080/19443994.2012.749054.

[19] N. Hilal, G. J. Kim, and C. Somerfield, 'Boron removal from saline water: A comprehensive review', Desalination, vol. 273, no. 1, pp. 23–35, 2011, doi: 10.1016/j.desal.2010.05.012.

[20] J. Wolska and M. Bryjak, 'Methods for boron removal from aqueous solutions - A review', Desalination, vol. 310, pp. 18–24, 2013, doi: 10.1016/j.desal.2012.08.003.

[21] A. A. Halim, N. A. Roslan, N. S. Yaacub, and M. T. Latif, 'Boron removal from aqueous solution using curcumin-impregnated activated carbon', Sains Malays, vol. 42, no. 9, pp. 1293–1300, 2013.

[22] C. Irawan, J. C. Liu, and C. C. Wu, 'Removal of boron using aluminum-based water treatment residuals (Al-WTRs)', Desalination, vol. 276, no. 1–3, pp. 322–327, 2011, doi: 10.1016/j.desal.2011.03.070.

[23] Y. Inukai et al., 'Removal of boron(III) by N-methylglucamine-type cellulose derivatives with higher adsorption rate', Anal Chim Acta, vol. 511, no. 2, pp. 261–265, 2004, doi: 10.1016/j.aca.2004.01.054.

[24] J. F. García Martín, M. Cuevas, C. H. Feng, P. Á. Mateos, M. T. García, and S. Sánchez, 'Energetic valorisation of olive biomass: Olive-tree pruning, olive stones and pomaces', Processes, vol. 8, no. 5, 2020, doi: 10.3390/PR8050511.

[25] J. Nampeera, Y. K. Recepoğlu, and A. Yuksel, 'Valorization of olive tree pruning waste for potential utilization in lithium recovery from aqueous solutions', Biomass Conversion and Biorefinery, 2022, doi: 10.1007/s13399-022-02647-2.

[26] B. Rzig, F. Guesmi, M. Sillanpää, and B. Hamrouni, 'Biosorption potential of olive leaves as a novel low-cost adsorbent for the removal of hexavalent chromium from wastewater', Biomass Convers Biorefin, vol. 1, p. 3, doi: 10.1007/s13399-022-03356-6.

[27] M. Calero, A. Pérez, G. Blázquez, A. Ronda, and M. A. Martín-Lara, 'Characterization of chemically modified biosorbents from olive tree pruning for the biosorption of lead', Ecol Eng, vol. 58, pp. 344–354, 2013, doi: 10.1016/j.ecoleng.2013.07.012.

[28] S. Liu et al., 'Radiation synthesis and performance of novel cellulose-based microsphere adsorbents for efficient removal of boron (III)', Carbohydr Polym, vol. 174, pp. 273–281, Oct. 2017, doi: 10.1016/J.CARBPOL.2017.06.012.

[29] G. S. Chauhan, L. Guleria, and R. Sharma, 'Synthesis, characterization and metal ion sorption studies of graft copolymers of cellulose with glycidyl methacrylate and some comonomers', Cellulose, vol. 12, no. 1, pp. 97–110, 2005, doi: 10.1007/s10570-004-2720-4.

[30] Y. Tang, Q. Ma, Y. Luo, L. Zhai, Y. Che, and F. Meng, 'Improved synthesis of a branched poly(ethylene imine)-modified cellulose-based adsorbent for removal and recovery of Cu(II) from aqueous solution', J Appl Polym Sci, vol. 129, no. 4, pp. 1799–1805, 2013, doi: 10.1002/app.38878.

[31] B. Rzig, F. Guesmi, M. Sillanpää, and B. Hamrouni, 'Modelling and optimization of hexavalent chromium removal from aqueous solution by adsorption on low-cost agricultural waste biomass using response surface methodological approach', Water Science and Technology, vol. 84, no. 3, pp. 552–575, 2021, doi: 10.2166/wst.2021.233.

[32] W. J. Liu, F. X. Zeng, H. Jiang, and X. S. Zhang, 'Preparation of high adsorption capacity bio-chars from waste biomass', Bioresources Technology, vol. 102, no. 17, pp. 8247–8252, 2011, doi: 10.1016/j.biortech.2011.06.014.

[33] M. I. El-Khaiary, 'Least-squares regression of adsorption equilibrium data: Comparing the options', J Hazard Mater, vol. 158, no. 1, pp. 73–87, Oct. 2008, doi: 10.1016/j.jhazmat.2008.01.052.

[34] S. K. Lagergren, 'About the theory of so-called adsorption of soluble substances', Sven. Vetenskapsakad. Handingarl, vol. 24, pp. 1–39, 1898.

[35] G. Blanchard, M. Maunaye, and G. Martin, 'Removal of heavy metals from waters by means of natural zeolites', Water Res, vol. 18, no. 12, pp. 1501–1507, Jan. 1984, doi: 10.1016/0043-1354(84)90124-6.

[36] I. Langmuir, 'The adsorption of gases on plane surfaces of glass, mica and platinum', J Am Chem Soc, vol. 40, no. 9, pp. 1361–1403, Sep. 1918, doi: 10.1021/JA02242A004/ASSET/JA02242A004.FP.PNG_V03.

[37] H. M. A. Freundlich, 'Concerning adsorption in solutions', J. Phys. Chem, vol. 57, p. 385, 1906.

[38] M. L. Nallappan, M. M. Nasef, T. M. Ting, and A. Ahmad, 'An Optimized Covalent Immobilization of Glucamine on Electrospun Nanofibrous Poly(vinylidene fluoride) Sheets Grafted with Oxirane Groups for Higher Boron Adsorption', Fibers and Polymers, vol. 19, no. 8, pp. 1694–1705, 2018, doi: 10.1007/s12221-018-8110-6.

[39] T. S. Anirudhan and P. Senan, 'Adsorption characteristics of cytochrome C onto cationic Langmuir monolayers of sulfonated poly(glycidylmethacrylate)-grafted cellulose: Mass transfer analysis, isotherm modeling and thermodynamics', Chemical Engineering Journal, vol. 168, no. 2, pp. 678–690, 2011, doi: 10.1016/j.cej.2011.01.056.

[40] J. Chen et al., 'Structure, Morphology, Thermostability and Irradiation-Mediated Degradation Fractions of Hemicellulose Treated with Γ-Irradiation', Waste Biomass Valorization, vol. 7, no. 6, pp. 1415–1425, Dec. 2016, doi: 10.1007/S12649-016-9489-1.

[41] M. Xu, Y. Ao, S. Wang, J. Peng, J. Li, and M. Zhai, 'Efficient adsorption of 1-alkyl-3-methylimidazolium chloride ionic liquids onto modified cellulose microspheres', Carbohydr Polym, vol. 128, pp. 171–178, 2015, doi: 10.1016/j.carbpol.2015.04.018.

[42] S. A. Ali, S. A. Mubarak, I. Y. Yaagoob, Z. Arshad, and M. A. J. Mazumder, 'A sorbent containing pH-responsive chelating residues of aspartic and maleic acids for mitigation of toxic metal ions, cationic, and anionic dyes', RSC Adv, vol. 12, no. 10, pp. 5938–5952, 2022, doi: 10.1039/d1ra09234k.

[43] T. K. Saha, N. C. Bhoumik, S. Karmaker, M. G. Ahmed, H. Ichikawa, and Y. Fukumori, 'Adsorption of Methyl Orange onto Chitosan from Aqueous Solution', J Water Resour Prot, vol. 02, no. 10, pp. 898–906, 2010, doi: 10.4236/jwarp.2010.210107.

[44] M. Khashij, P. Mohammadi, M. Babei, M. Mehralian, and N. Aghamohammadi, 'Process optimization and modeling of lead removal using maleate/PAN nanocomposite nanofibers: Characterization, kinetics and isotherm studies', Desalination Water Treat, vol. 210, pp. 330–339, Jan. 2021, doi: 10.5004/dwt.2021.26537.

[45] X. Li, R. Liu, S. Wu, J. Liu, S. Cai, and D. Chen, 'Efficient removal of boron acid by N-methyl-d-glucamine functionalized silica-polyallyamine composites and its

adsorption mechanism', J Colloid Interface Sci, vol. 361, no. 1, pp. 232–237, 2011, doi: 10.1016/j.jcis.2011.05.036.

[46]   T. M. Ting et al., 'Comparative modelling analysis of boron dynamic adsorption on fibrous adsorbent prepared using radiation grafting versus granular resin', J Environ Chem Eng, vol. 9, no. 3, p. 105208, Jun. 2021, doi: 10.1016/J.JECE.2021.105208.

[47]   X. Zhang et al., 'A spherical N-methyl-d-glucamine-based hybrid adsorbent for highly efficient adsorption of boric acid from water', Sep Purif Technol, vol. 172, pp. 43–50, Jan. 2017, doi: 10.1016/J.SEPPUR.2016.08.002.

[48]   J. H. van't Hoff, 'JH Etudes de dynamique chimique', Frederik Muller & Co., Amsterdam, 1884.

[49]   A. Baba et al., 'Hydrogeology and hydrogeochemistry of the geothermal systems and its direct use application: Balçova-Narlıdere geothermal system, İzmir, Turkey', Geothermics, vol. 104, no. February, 2022, doi: 10.1016/j.geothermics.2022.102461.